Inflammation, Vol. 42, No. 6, December 2019 (© 2019)
DOI: 10.1007/s10753-019-01074-2

ORIGINAL ARTICLE

GSK-3β Inhibitor Induces Expression of the TLR4/MyD88/NF-κB Signaling Pathway to Protect Against Renal Ischemia-Reperfusion Injury During Rat Kidney Transplantation

Shuai Su,[1] Peng Zhang,[2] Qilin Zhang,[1] and Zhikang Yin[1,3]

Abstract— Ischemia-reperfusion injury (IRI) is an inevitable consequence of kidney transplantation (KT). The aim of our study was to investigate the protective effect of a glycogen synthase kinase 3β (GSK-3β) inhibitor against cold IRI in a rat renal transplantation (RT) model and a rat cold-IRI model through the toll-like receptor 4 (TLR4)/myeloid differentiation factor 88 (MyD88)/nuclear factor κ-light-chain-enhancer of the activated B cell (NF-κB) signaling pathway. We treated Sprague Dawley (SD) rats in the RT and cold-IRI models with 5 mg/kg and 1 mg/kg, respectively, of the GSK-3β inhibitor 4-benzyl-2-methyl-1,2,4-thiadiazolidine-3,5-dione (TDZD-8). We then measured inflammatory factors, *i.e.*, tumor necrosis factor alpha (TNF-α) and interleukins-1β and IL-6 (IL-1β, IL-6), as well as oxidative stress markers, *i.e.*, superoxide dismutase (SOD) and malondialdehyde (MDA), in serum and kidneys. Renal function tests and pathological examinations were performed at 0, 1, 2, 3, and 7 days after RT or cold IRI. We measured expression of TLR4, MyD88, inhibitor of NF-κB kinase (IκB), phosphorylated IκB (p-IκB), NF-κB p65, p-p65, GSK-3β, and phosphorylated GSK-3β (p-GSK-3β) by Western blot and immunohistological staining. After intervention with the GSK-3β inhibitor, renal function was improved; oxidative stress injury was reduced; expression of p-GSK-3β was upregulated; expression of p-IκB, TLR4, MyD88, and p-p65 was downregulated; pathological damage was significantly reduced; and expression of TNF-α, IL-1β, and IL-6 messenger ribonucleic acid (mRNA) was downregulated. These results strongly suggested that GSK-3β might be a key target for the treatment of IRI in KT. The GSK-3β inhibitor inhibited phosphorylation of NF-κB p65 and IκB by inhibiting the TLR/MyD88 pathway, reducing oxidative stress injury and the production of downstream inflammatory factors.

KEY WORDS: glycogen synthase kinase 3β; TLR4/MyD88/NF-κB pathway; renal ischemia-reperfusion injury; kidney transplantation.

Shuai Su and Peng Zhang contributed equally to this work.

[1] Department of Urology, The First Affiliated Hospital of Chongqing Medical University, Yixueyuan Road 1#, Yuzhongqu, Chongqing, 400016, China
[2] Department of Forensic Medicine, Hainan Medical University, Haikou, 571199, China
[3] To whom correspondence should be addressed at Department of Urology, The First Affiliated Hospital of Chongqing Medical University, Yixueyuan Road 1#, Yuzhongqu, Chongqing, 400016, China. E-mail: yinzhikang2005@sina.com

INTRODUCTION

As the number of patients with chronic kidney disease increases, kidney transplantation (KT) has become the best treatment for end-stage nephropathy [1]. Among the variables that affect the prognosis of the transplanted kidney, one important risk factor is ischemia-reperfusion injury (IRI). When the kidney is preserved in cryopreservation fluid for a long time, it will undergo cold ischemia. About 30% of delayed graft dysfunctions after KT are caused by cold IRI [2, 3]. Therefore, IRI is an important process during KT that seriously affects the early and delayed functions of a renal allograft. Although different types of drugs and molecules have been reported in the prevention and treatment of renal IRI, the clinical efficacy of drugs is not good.

The glycoprotein synthase kinase 3 (GSK-3) family consists of 2 subtypes, GSK-3α and GSK-3β, which play important roles in the repair and injury of renal tubular epithelial cells [4]. Researchers have found that GSK-3β participates in the regulation of multiple cellular functions, such as insulin signaling, apoptosis, cellular proliferation and division, and embryonic development [5]. The inhibitory effect of GSK-3β inhibitors on nuclear factor κ-light-chain-enhancer of activated B cell (NF-κB) transcription has been demonstrated in a recent study [6]. Toll-like receptors (TLRs) are a family of transmembrane proteins produced constitutively in renal cells; their activation results in transport of NF-κB from the cytoplasm to the nucleus, resulting in overexpression of inflammatory cytokines and thus pro-inflammatory responses [7]. Inhibiting GSK-3β significantly increases the production of pro-inflammatory cytokines and inhibits the release of inflammatory cytokines stimulated with TLR ligands [8]. It is reported that TLR4 plays an indispensable role in the pathogenesis of renal IRI, which is inevitable during KT [9]. Two signaling pathways are involved in TLR4 signal transduction: the myeloid differentiation factor 88 (MyD88)-dependent pathway and the TIR domain-containing adaptor protein inducing IFN-β (TRIF)-dependent pathway [10]. The TLR4/MyD88 pathway mediates the release of pro-inflammatory cytokines [11]. Normally, NF-κB is stable in the cytoplasm but is inactive and does not function to transcribe genes. NF-κB dimers are retained in the cytoplasm in inactive form through interaction with NF-κB kinase (IκB) proteins. External stimuli such as bacteria, viruses, viral metabolites, or cytokines can induce IκB phosphorylation, ubiquitination, and nuclear translocation; this leads to the entry of p65/p50 heterodimer into the nucleus, causing transcription of related genes [12]. But this mechanism has not been confirmed in KT.

GSK-3β inhibitors have been demonstrated to protect against organ damage in several animal models [13]. Currently, there are no specific treatments to prevent cold IRI in clinical KT. In addition, the role of the TLR4/MyD88/NF-κB signaling pathway in KT remains to be elucidated. In our study, we applied a GSK-3β inhibitor to a rat renal transplantation (RT) model and rat cold IRI model to observe its protective effect against renal IRI and its mechanism of action. We expect GSK-3β inhibitors in general to become new targets of research in the treatment of IRI in KT.

MATERIALS AND METHODS

Animal Studies

All animal procedures for this study were performed strictly according to the *Guide for the Care and Use of Laboratory Animals* and were approved by the Animal Care and Use Committee of Chongqing Medical University, Chongqing, China. We used a total of 48 male Sprague Dawley (SD) adult rats weighing at least 250 g each as both kidney donors and recipients. Food and water were available *ad libitum*, although the animals were deprived of food but not water 12 h before surgery. Anesthesia was induced and maintained with pentobarbital (30 g/L, 300 mg/kg; Sigma-Aldrich, St. Louis, MO, USA) *via* intraperitoneal injection.

Establishment of Animal Models

We established 2 different rat models, cold IRI and RT. Our cold IRI model was established to simulate KT. Both models received the same dose of drug intervention.

Cold IRI Model

Rats were divided into the following groups ($n = 6$ each): (1) sham operation group; (2) cold IRI group without intervention, undergoing the operation described below; (3) 5 mg/kg 4-benzyl-2-methyl-1,2,4-thiadiazolidine-3,5-dione (TDZD-8) + cold IRI group; (4) 1 mg/kg TDZD-8 + cold IRI group. In the TDZD-8 group, rats were given

intravenous (i.v.) TDZD-8 5 min before we closed the abdominal cavity. In the sham and cold IRI-only groups, rats were given 10% dimethyl sulfoxide (DMSO; 1 mL/kg) dissolved in normal saline (NS; i.v.) 5 min before we closed the abdominal cavity.

RT Model

Rats were divided into the following 4 groups ($n = 6$ each): (1) sham operation group; (2) RT-only group: these rats received vehicle (10% DMSO dissolved in NS, 1 mL/kg, i.v.) 5 min before receiving transplanted kidneys; (3) 5 mg/kg TDZD-8 + RT group; (4) 1 mg/kg TDZD-8 + RT group. In the TDZD-8 groups, rats were given TDZD-8 (i.v.) 5 min before recipients received KT.

RT Model

In donor rats, we used a midline laparotomy incision to enter the abdominal cavity and then bluntly separated the perirenal fat from the tissue. Both kidneys (with ureters and vascular pedicles) were placed into a treatment plate with cold saline (0 °C) for 1 h. In recipient rats, the renal artery was anastomosed end-to-side to the abdominal aorta, distal to the renal arteries, and proximal to the bifurcation. We performed end-to-end venous anastomosis with an 8-0 nylon suture between the graft and the recipient renal vein, and then we used the bladder flap anastomosis technique to suture the ureter [14]. Right recipient nephrectomy was performed immediately after KT (Fig. 1(A–G)).

Cold IRI Model

After administering abdominal anesthesia to the rats, we made a median incision in the abdomen, and then we pushed the intestines to the right in order to free the left kidney and left renal artery, vein, and abdominal aorta. Next, we clamped the upper and lower ends of the abdominal aorta and inferior renal vena cava with non-traumatic vascular clamps. The upper-end clamp was higher than the opening of the left renal artery on the abdominal aorta; the lower-end clamp was lower than the opening of the corresponding right renal artery. Ringer's lactate (RL) solution with heparin (25 U/L) was slowly and uniformly perfused into the right renal artery using a 5-mL injector; the left adrenal vein was used as the outlet for the perfusion fluid. We performed continuous perfusion until the effluent was clear and the left kidney was pale. We ligated the right renal pedicle, removed the right kidney, and clipped the left renal artery and vein with a non-invasive blood vessel clamp. The left kidney was put into a homemade kidney bag of RL solution (0 °C). After 1 h, all clips were removed to restore blood flow to the left kidney (Fig. 1(A1–G1)).

Measurement of Oxidative Stress Biomarkers (SOD, MDA)

After flushing the tissue with a precooled phosphate-buffered saline (PBS) to remove residual blood, we mixed it with 100 mmol/L tris hydrochloride (tris-HCl) buffer and homogenized it at 10,000*g* for 20 min. Coomassie Brilliant Blue staining was used to determine the total protein concentration. We measured superoxide dismutase (SOD) and malondialdehyde (MDA) contents using commercial kits (Xinfan Biotechnology, Shanghai, China).

Evaluation of NF-κB, TLR4, MyD88, IκB, and GSK-3β Activity

Immunohistochemical Staining

We used immunohistochemical (IHC) with anti-p65 and anti-GSK-3β antibodies (Cell Signaling Technology [CST], Danvers, MA, USA) to examine expression of p65 and GSK-3β in rat renal tissue. The wax block of the kidney tissue was divided into 5-μm slices. After being dried and dewaxed, the kidney slices were repaired with citrate after each concentration gradient of dimethylbenzene and ethanol. Finally, we perfused the slices with H_2O_2 in order to clear endogenous hydrogen peroxidase. Samples were then incubated with antibody (p65, 1:100 dilution; GSK-3β, 1:100 dilution) overnight at 4 °C. After washing them with PBS, we added goat anti-mouse antibody (Bioss, Beijing, China), incubated the sections for 30 min at 37 °C, and stained them with dDAB (Boster Biological Technology, Ltd., Wuhan, China) for 2 min. Staining was considered positive when brownish-yellow particles occurred in tissue. Finally, we used Image-Pro Plus software version 6.0 (Media Cybernetics, Inc., Rockville, MD, USA) to determine the cumulative light density of the positive region.

Determination of Protein Concentration by Western Blot

Via Western blot, we detected p-p65, p-GSK-3β, GSK-3β, p65 (CST), MyD88, (Abcam, Cambridge, UK), IκB, p-IκB, and TLR4 (Santa Cruz Biotechnology, Dallas, TX, USA) contents in rat kidney tissue. We used β-actin (Abcam) and glyceraldehyde 3-phosphate dehydrogenase (GAPDH; Santa Cruz) as loading controls. The kidney tissue in each group was homogenized on ice (0 °C), and

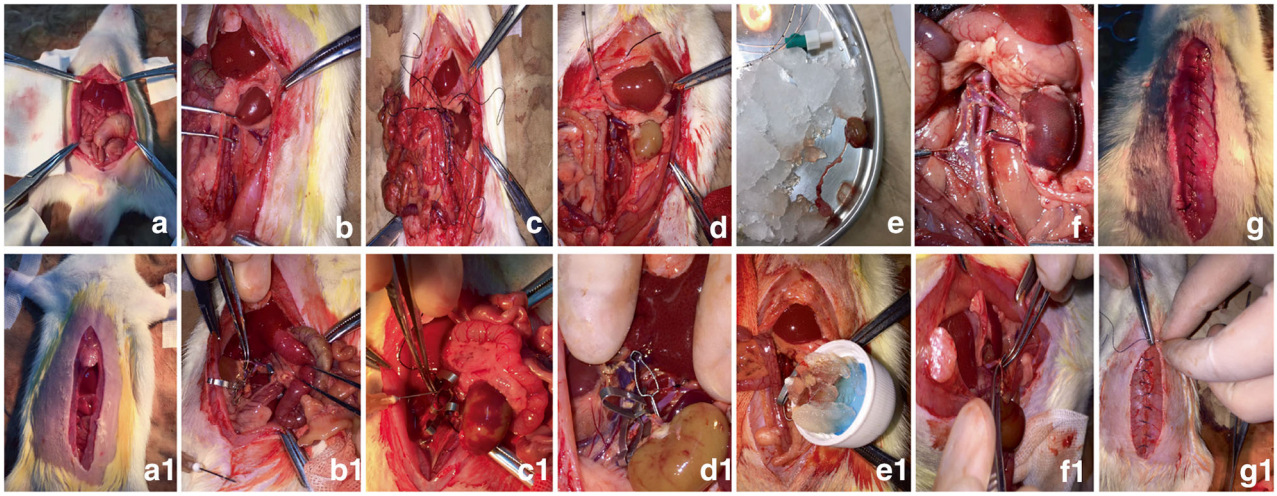

Fig. 1. Establishment of (A–G) rat RT model and (A1–G1) rat cold IRI model. (A) Middle abdominal incision. (B) Blunt separation of ureter. (C) Blunt separation of blood vessel. (D) Perfusion (RL solution). (E) The left kidney was stored in NS (0 °C) for 1 h. (F) Vascular anastomosis (vein: end-to-end anastomosis; artery: end-to-side anastomosis). (G) Closing the abdominal cavity. (A1) Middle abdominal incision. (B1) Blunt separation of renal artery and vein. (C1) Perfusion from the right renal artery. (D1) Clipping renal artery and vein with non-invasive vascular clamp. (E1) The left kidney was stored at NS (0 °C) for 1 h. (F1) The right kidney was removed. (G1) Closing the abdominal cavity.

nuclear protein was extracted using a Nuclear Protein Extraction Kit (Beyotime Institute of Biotechnology, Shanghai, China). A part of rat kidney tissue samples was homogenized in ice-cold RIPA lysis buffer (Beyotime) with 1 mM PMSF (Beyotime). The protein sample was resolved by sodium dodecyl sulfate-polyacrylamide gel electrophoresis (SDS-PAGE) and transferred to polyvinylidene difluoride (PVDF) membranes. Then, we blocked the membranes with 5% nonfat milk for 2 h and incubated them with primary antibody overnight at 4 °C. After subsequently washing them with tris-buffered saline + Polysorbate 20 (TBST), we incubated the membranes with a peroxidase-conjugated secondary antibody (1:2000; Bioss) and visualized results using an electrochemiluminescence (ECL) system (Bioss).

Pathological Section (Hematoxylin and Eosin) and Renal Tubular Necrosis Score

We divided the wax block of the kidney tissue into 5-μm slices, dewaxed and dehydrated them, dyed them with hematoxylin and eosin (H&E), and observed changes in renal histology under a microscope (Olympus Microscopy, Tokyo, Japan), viewing areas with serious tissue lesions under high magnification (× 400). We used 100 renal tubules with 10 high-magnification visual fields for renal tubule score according to Paller's method.

Enzyme-Linked Immunosorbent Assay

Abdominal aortic blood was taken from rats in each group 24 h post-operation, and the supernatant was obtained by centrifuging the blood at 3000 r/min for 15 min at room temperature. We performed an enzyme-linked immunosorbent assay (ELISA) on the supernatant using an ELISA kit (R&D Systems, Minneapolis, MN, USA) per manufacturer's instructions: we incubated the ELISA plate with sample and antibody working fluid at 37 °C for 60 min, washed it with PBS 3–5 times, and then added enzyme-labeled reagent to terminate the reaction. We determined absorbance at 450 nm (optical density [OD] 450) and detected expression levels of IL-6, IL-1β, and TNF-α in serum using a microplate reader (BioTek, Winooski, VT, USA).

Quantitative Real-Time Polymerase Chain Reaction

We isolated total ribonucleic acid (RNA) of rat kidney tissue using TRIzol Reagent (Takara, Otsu, Japan) and determined RNA concentration by spectrophotometry. Single-stranded complementary deoxyribonucleic acid (cDNA) was synthesized using a quantitative real-time polymerase chain reaction (RT-qPCR) kit (Thermo Fisher Scientific, Waltham, MA, USA). We measured cDNA in 96-well plates in duplicate using an SYBR Green I kit (Takara). The primers used for the assays are presented in

Table 1. For each sample, relative gene expression was calculated using the comparative 2−ΔΔCt method with the GAPDH as a reference.

Statistical Analysis

We used SPSS software version 22.0 (SPSS, Inc., Chicago, IL, USA) to carry out statistical analysis. Experimental data are presented as the mean ± standard error of the mean (SEM). $P < 0.05$ was considered statistically significant. We performed univariate assessment of categorical variables using Student's *t* test, one-way analysis of variance (ANOVA), and chi-squared test.

RESULTS

Renal Function Test in RT and Cold IRI Models

To investigate the therapeutic effects of GSK-3β inhibition, we performed a time-history analysis of rat serum creatinine (SCr) and blood urea nitrogen (BUN) levels, the results of which are shown in Fig. 2. In both the RT and cold IRI models, levels of SCr and BUN increased significantly on day 1 and began to decrease starting on day 2. After TDZD-8 intervention, SCr and BUN levels significantly decreased on days 1, 2, and 3, compared with the RT-only or cold IRI-only group. However, in the RT model, the BUN level decrease in the RT + 5 mg/kg TDZD-8 group from the baseline level of the RT-only group was greater than the corresponding decrease in the RT + 1 mg/kg TDZD-8 group on days 2 and 3. In the cold IRI model, there was no obvious decrease in BUN levels in the cold IRI + 1 mg/kg TDZD-8 group compared with the cold IRI-only group on day 3, which showed that 5 mg/kg TDZD-8 protected renal function better than 1 mg/kg TDZD-8 did. There was no significant difference in the decrease in SCr level between the 5 and 1 mg/kg TDZD-8 groups in either animal model.

Table 1. Primers Used for the Assays

TNF-α	
Forward	5′-CTG AAC GAA TTC GGG GTG ATC GG-3′
Reverse	5′-GGC TTG TCA CTC GAA-3′
IL-1β	
Forward	5′-ACT ATG GCA ACT GTC CCT GAAC-3
Reverse	5′-GTG CTT GGG TCC TCA TCC TG-3′
IL-6	
Forward	5′-TTC CTC TGG TCT TCT GGA GT-3′
Reverse	5′-TGT GAC TCC AGC TTA TCT CTT GG-3′
GAPDH	
Forward	5′-GGT CAC CAG GGC TGC CAT TTG-3′
Reverse	5′-CTG GTA CTC CAT ACA CTG GCT-3′

Effect of GSK-3β Inhibitor on Inflammatory Factors

We waited 24 h post-surgery to detect changes in inflammatory factors in rat arterial blood. Serum levels of pro-inflammatory cytokines were significantly increased in the cold IRI and RT groups compared with the sham group. Compared with RT-only and cold IRI-only groups, levels of inflammatory cytokines were significantly lower in TDZD-8 groups. There was no statistically significant difference between the 2 TDZD-8 treatment groups in either the RT model or the cold IRI model. The RT + 5 mg/kg TDZD-8 group showed a decrease in the IL-6 level, but it was not statistically significant (Fig. 3).

As shown in Fig. 3d, TNF-α, IL-6, and IL-1β mRNA expression was higher in the RT and cold IRI groups than in the sham group. Interestingly, the increase in IL-6, TNF-α, and IL-1β mRNA levels was remarkably attenuated in the TDZD-8 groups compared with the RT-only and cold IRI-only groups, which was consistent with ELISA results.

The Effect of GSK-3β Inhibitor on Renal Pathological Changes

Figures 4 and 5 display a time-history analysis of renal pathological changes as shown by H&E staining. Rat kidney tissue taken from the sham group at each time point (days 0, 1, 2, 3, and 7) had normal tubular histology. Rats that had undergone either RT or cold IRI demonstrated severe pathological damage such as interstitial congestion, cell exfoliation and necrosis, visible protein casts, glomerular structural damage, and inflammatory cell infiltration. The most severe pathological injuries occurred on days 1 and 2. Histological changes were significantly reduced in TDZD-8 treatment groups in both models on days 1, 2, 3, and 7. In these groups, we observed a marked reduction in renal tubular epithelial cell necrosis and interstitial hyperemia; furthermore, reduction of pathological damage in the 5 mg/kg group was greater than that in the 1 mg/kg group. However, compared with the sham group, both the cold IRI and RT groups showed a significant change in the renal tubular necrosis score, which decreased significantly on day 1 and remained lower until day 7 after treatment with TDZD-8 (Fig. 6).

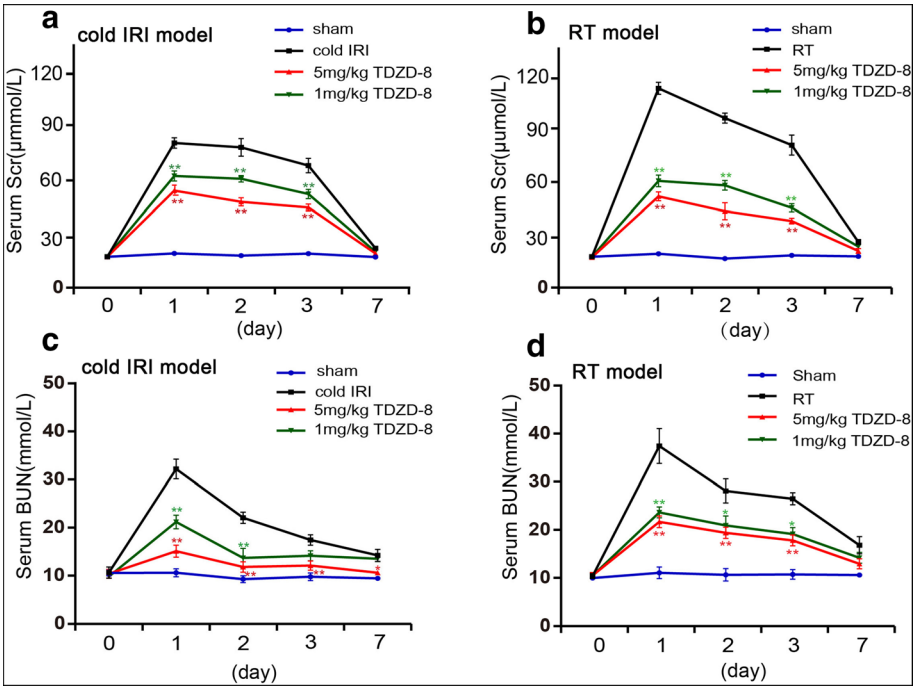

Fig. 2. Serum levels of SCr and BUN on days 0, 1, 2, 3, and 7. **a** SCr content in rat cold IRI model. **b** SCr content in rat RT model. **c** BUN content in rat cold IRI model. **d** BUN in rat RT model. $*P < 0.05$, $**P < 0.01$ compared with RT group or cold IRI group; $n = 6$ rat/group.

Effect of GSK-3β Inhibitor on GSK-3β

In both the RT and cold IRI models, expression of p-GSK-3β in kidney tissue from either the RT or cold IRI group was significantly reduced compared with the sham group. After treatment with TDZD-8, p-GSK-3β levels significantly increased in both the 5 mg/kg and 1 mg/kg TDZD-8 treatment groups *vs.* the cold IRI-only or RT-only group, and the increase in p-GSK-3β in the 5 mg/kg TDZD-8 group was higher than that in the 1 mg/kg TDZD-8 group. However, total GSK-3β levels remained unchanged (Fig. 7).

IHC results showed that sites positive for GSK-3β were mainly in the cytoplasm of renal tubules and some glomerular epithelial cells (Fig. 8). The sham group was very weakly positive for expression of GSK-3β. By contrast, staining was significantly greater in the tubulointerstitium of the kidneys in the RT and cold IRI groups. TDZD-8 reduced the expression of GSK-3β, but in the 2 TDZD-8 treatment groups of the RT model, this decrease was not statistically significant (Fig. 8c). In the cold IRI model, however, GSK-3β expression was more greatly reduced in the 5 mg/kg TDZD-8 group than in the 1 mg/kg TDZD-8 group.

GSK-3β Inhibitor Regulated Inflammatory Responses by Blocking TLR4/MyD88/NF-κB Pathway Activation

To determine the role of TLR4 in the development of IRI, we examined its expression in the renal tissue of the RT group. A time-course analysis of renal TLR4 expression is shown in Fig. 9c. TLR4 expression was significantly increased in kidney tissue 24 h after induction of ischemia and reperfusion in the RT model, after which it decreased gradually.

We investigated whether GSK-3β inhibition exerted its effects through the TLR4/MyD88/NF-κB signaling pathway. In the RT model, compared with the sham group, the RT groups showed a significant increase in expression of TLR4, MyD88, p-IκB, and p-p65. However, such expression was significantly decreased after intervention with TDZD-8, and there was no significant difference in dose contrast between the 2 TDZD-8 groups. In the cold IRI model, there was a significant increase in TLR4, MyD88, p-IκB, and p-p65 expression; after TDZD-8 intervention, such expression was significantly decreased (Fig. 9).

IHC results for p65 showed that positive sites were mainly in the cytoplasm and nuclei of renal tubules (Fig. 8).

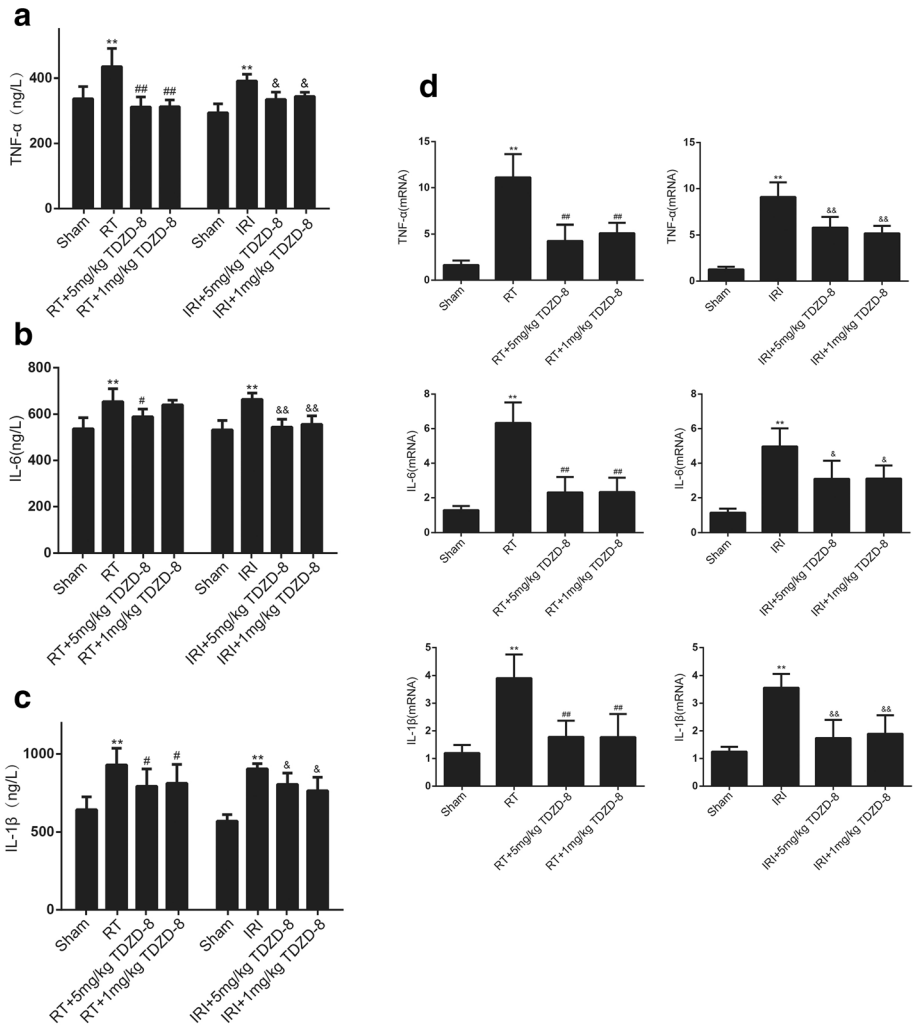

Fig. 3. GSK3β inhibition reduced pro-inflammatory cytokines following RT and cold IRI. Effect of TDZD-8 administration (RT model, 5 mg/kg; cold IRI model, 1 mg/kg; i.v.) on serum levels of **a** TNF-α, **b** IL-6, and **c** IL-1β. **d** The relative expression mRNA levels of TNF-α, IL-1β, and IL-6 were detected by RT-qPCR. $^{*}P < 0.05$ *vs.* sham group, $^{**}P < 0.01$; $^{\#}P < 0.05$ *vs.* RT group, $^{\#\#}P < 0.01$; $^{\&}P < 0.05$ *vs.* cold IRI group, $^{\&\&}P < 0.01$.

There was almost no p65 expression in the sham group of either the RT or cold IRI model; it was mainly expressed in the cytoplasm and nuclei of renal tubular epithelial cells in the RT and cold IRI groups. Compared with the RT-only and cold IRI-only groups, the TDZD-8 groups in each model showed a significant reduction in nuclear displacement of renal tubular epithelial cells in cytoplasm and nuclei. The expression level of p65 in the 5 mg/kg TDZD-8 group was significantly lower than that in the 1 mg/kg TDZD-8 group (Fig. 8d).

Effect of TDZD-8 on MDA and SOD

Results showed that in both animal models, renal SOD activity in the cold IRI and RT groups was lower than that in the sham group (Fig. 8e), while the MDA content was higher (Fig. 8f). In both models, SOD activity increased and the MDA content decreased after treatment with TDZD-8. There was no statistically significant difference in the reduction of MDA between the 5 mg/kg and 1 mg/kg TDZD-8 groups, but only the 5 mg/kg TDZD-8 group showed a significant increase in SOD expression.

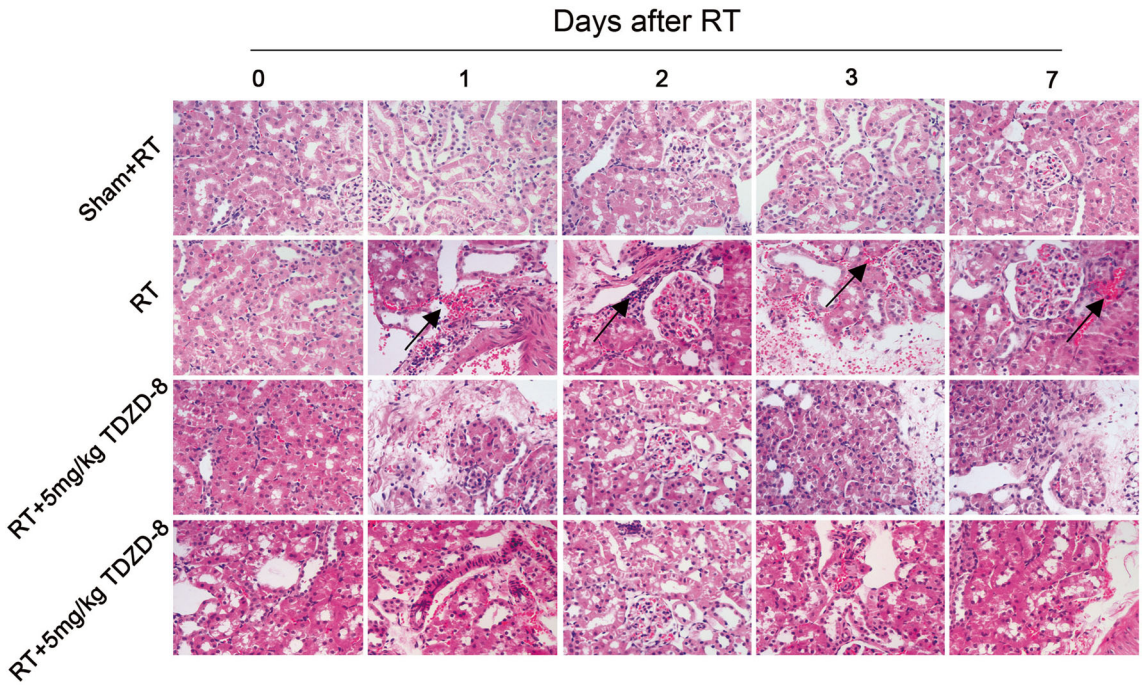

Fig. 4. Pathological changes in rat RT model on days 0, 1, 2, 3, and 7 (H&E-stained; × 200). Black arrowhead: pathological damage (hemorrhage, necrosis of renal tubular epithelial cells, infiltration of inflammatory cells, loss of brush border). After intervention with TDZD-8, pathological damage was reduced significantly (at both 5 mg/kg and 1 mg/kg, but 5 mg/kg had a better effect).

DISCUSSION

In our study, we identified the protective effect of the GSK-3β inhibitor against acute kidney injury after KT. First, GSK-3β has a certain inhibitory effect on TLR4 through the MyD88-dependent signaling pathway, which protects against renal IRI after KT. Second, the GSK-3β inhibitor could protect against IRI by inhibiting NF-κB activation; at the same time, it could also protect kidney function by reducing oxidative stress injury.

Cold IRI plays an indispensable role in the development of renal function injury and chronic allograft nephropathy after KT [15, 16]; renal IRI further worsens inflammation and oxidation [17]. Therefore, we studied IRI from both a simple cold IRI model (with IRI as the single factor) and a complicated RT model (with multiple factors such as IRI and immune rejection) to prove that the simpler cold IRI model could replace the more complex RT model.

Recent studies have shown that inhibiting GSK-3β could alleviate inflammation in brain endothelial cells and reduce levels of acute systemic inflammatory cytokines [18, 19]. Ren showed that GSK-3β activation increases in IRI and that pharmacological inhibitors can inhibit activity of this enzyme [20]. Highly selective GSK-3β inhibitors have been shown to suppress NF-κB activation, inhibit the TLR/MyD88 signaling pathway, reduce multiple-organ injury, and alleviate acute systemic inflammatory responses [6, 21]. TLR4/MyD88 and NF-κB are upstream and downstream signal transduction pathways that play indispensable roles in initiating cell inherent immunoresponses [22, 23]. Finally, TLR4 regulates the release of various inflammatory factors by increasing the expression of its downstream factors, thereby causing damage to the body [24]. Mice with a genetic deficiency in TLR4 or the adaptor molecule MyD88 were shown to be protected from renal insufficiency and histological damage [25].

TLR4 signaling occurs through the TRIF- and MyD88-dependent pathways. The TLR/MyD88 signaling pathway plays a leading role in IRI-mediated renal injury [26]. We assessed the association between the TLR4/MyD88 pathway and acute kidney injury in our rat RT and cold IRI models. The TLR4/MYD88/NF-κB pathway has been found to form a signal axis and participate in inflammatory response [27]. TLR4 binds to the adaptor molecule MyD88 and activates IKK–IκB–NF-κB by a series of cascade reactions, whereupon NF-κB is activated

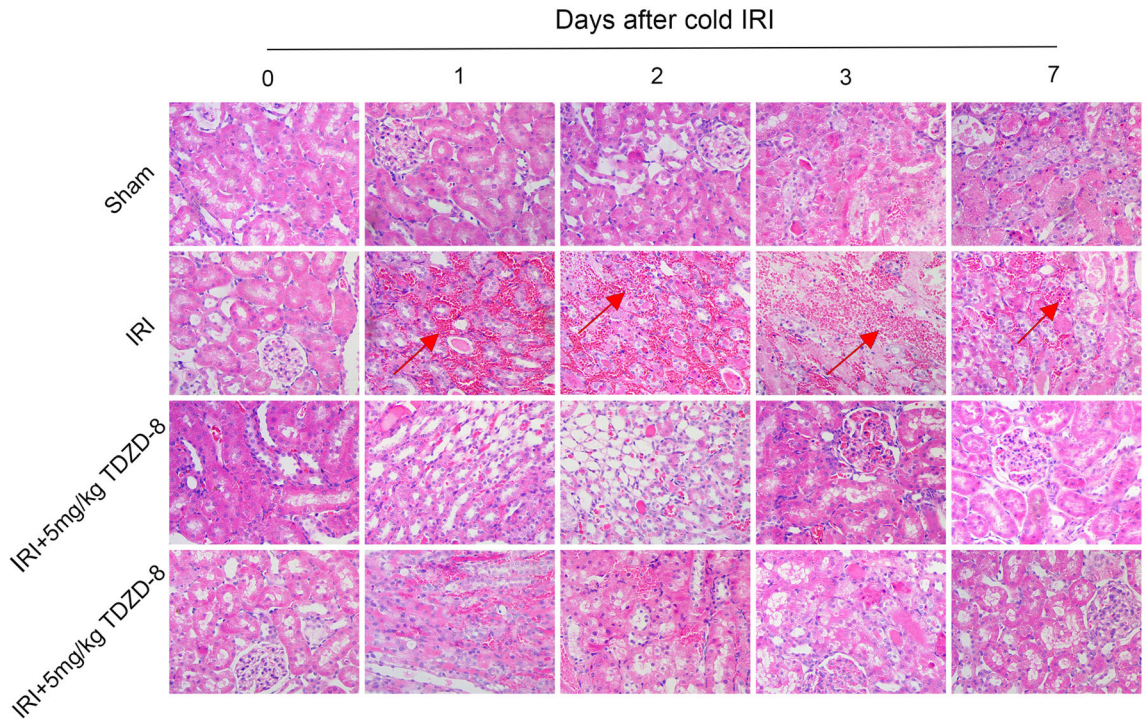

Fig. 5. Pathological changes in the rat cold IRI model on days 0, 1, 2, 3, and 7 (H&E-stained; × 200). Red arrowhead: pathological damage (bleeding, inflammatory cell infiltration, loss of brush border). After intervention with TDZD-8, pathological damage was reduced significantly (at both 5 mg/kg and 1 mg/kg, but 5 mg/kg had a better effect).

by nuclear localization sequence (NLS) from the cytoplasm to the nucleus. κB can be bound to specific κB sequences on target genes, subsequently synthesizing and releasing TNF-α, IL-1, and other inflammatory factors.

The GSK-3β inhibitor has been shown to reduce kidney, lung, neuromuscular, and liver injury as well as systemic release of pro-inflammatory cytokines. Inhibiting GSK-3β activity downregulates the activation of the TLR4/MyD88/NF-κB pathway and inhibits production of inflammatory mediators [28, 29]. Various studies have reported that GSK-3β could affect TLR4/MyD88/NF-κB activity by several different mechanisms: (1) facilitating translocation of p50/p65 to the nucleus and binding to DNA, (2) p65 phosphorylation, (3) IκB phosphorylation, or (4) *via* cAMP-response element binding protein (CREB) [6, 30–32]. Schwabe et al. examined the amino acid

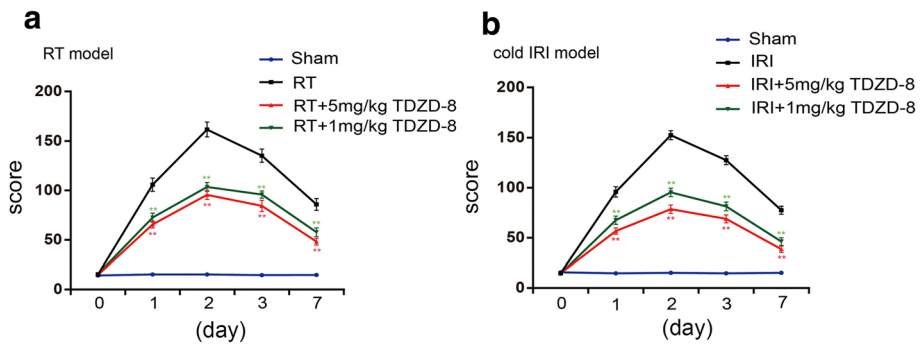

Fig. 6. Renal tubular necrosis score of rat **a** RT model and **b** cold IRI model on days 0, 1, 2, 3, and 7. Necrosis score reduced significantly on day 1, and this reduction lasted until day 7 after treatment with TDZD-8. $^{*}P < 0.05$, $^{**}P < 0.01$, compared with RT group or cold IRI group.

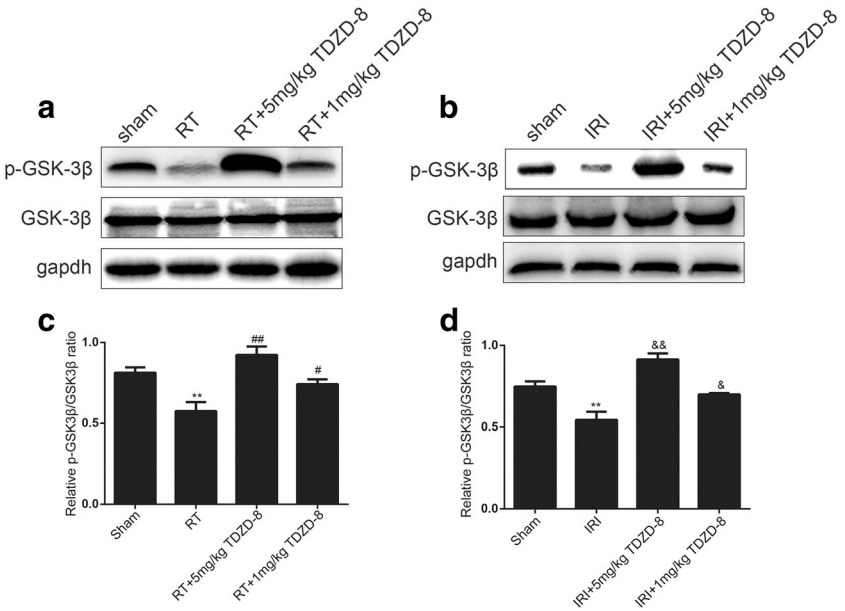

Fig. 7. The effects of TDZD-8 administration on GSK-3β phosphorylation of rat renal tissues at 24 h after ischemia-reperfusion as detected by Western blot. **a** Expression of p-GSK-3β and GSK-3β in the rat RT model. **b** Expression of p-GSK-3β and GSK-3β in the rat cold IRI model. **c**, **d** Densitometric analysis of the bands is expressed as the relative optical density (ROD) of p-GSK-3β, corrected with the corresponding total GSK-3β content. $^{*}P < 0.05$ *vs.* sham group, $^{**}P < 0.01$; $^{\#}P < 0.05$ *vs.* RT group, $^{\#\#}P < 0.01$; $^{\&}P < 0.05$ *vs.* cold IRI group, $^{\&\&}P < 0.01$.

sequence of RelA/p65 and proved that it contains a variety of potential phosphorylation consensus motifs of GSK-3β [33]. Recent studies [34] have shown that reperfusion injury stimulates NF-κB p65 Ser536 phosphorylation and promotes NF-κB activation.

We found that expression of TLR4 and its endogenous ligands increased after RT and that complete development of renal IRI depended on the TLR4/MyD88 signaling pathway. Our research confirmed that TDZD-8 significantly reduced phosphorylation of NF-κB p65 and IκB as well as expression of TLR4 and MyD88 in rat renal tissue. GSK-3β is usually active in the cell and plays a biological role *via* its phosphorylated downstream substrates. When an external stimulus is received, GSK-3β is phosphorylated to reduce its activity, thereby changing the activity and function of the downstream components. Consequently, we confirmed that TDZD-8 can significantly increase phosphorylation and reduce activity of GSK-3β. The binding of TLR4 to its ligands induces a variety of downstream effects, including activation and expression of pro-inflammatory cytokines [35]. Inflammatory factors such as IL-6, IL-1, TNF-α, and IL-8 are involved in the process of KT [36, 37]. IL-1 can induce neutrophils to infiltrate renal tissue, aggravating renal injury. TNF-α not only has direct cytotoxicity but also promotes the production of IL-1, IL-6, and other cytokines, creating an amplifying effect that aggravates the infiltration and aggregation of inflammatory cells [38]. In our study, levels of IL-6, IL-1β, and TNF-α increased significantly in cold IRI and RT groups compared with sham groups, suggesting that renal reperfusion can stimulate the formation of IL-6, IL-1β, and TNF-α. However, after treatment with TDZD-8, levels of all 3 cytokines plus SCr and BUN were significantly lower than in the cold IRI-only and RT-only groups. This indicated that TDZD-8 could be used as an anti-inflammatory substance to reduce release of TNF-α, IL-1β, and IL-6 induced by ischemia-reperfusion in RT, protect renal function, and exert an anti-inflammatory effect.

Oxyradicals and active oxygen play very important roles in IRI [39]. In the body, one system produces free radicals and another eliminates them, jointly maintaining oxidation-antioxidant balance [40]. One study found that a large number of oxygen free radicals produced by ischemia-reperfusion exceeded the scavenging ability of local tissues, resulting in tissue damage [41]. SOD is a scavenger of free radicals, and therefore, SOD levels can reflect an organism's ability to scavenge oxygen free radicals [42]; in addition, SOD activity can reflect the kidney's ability to resist lipid peroxidation [43]. MDA is a relatively stable metabolic intermediate in lipid peroxidation; the

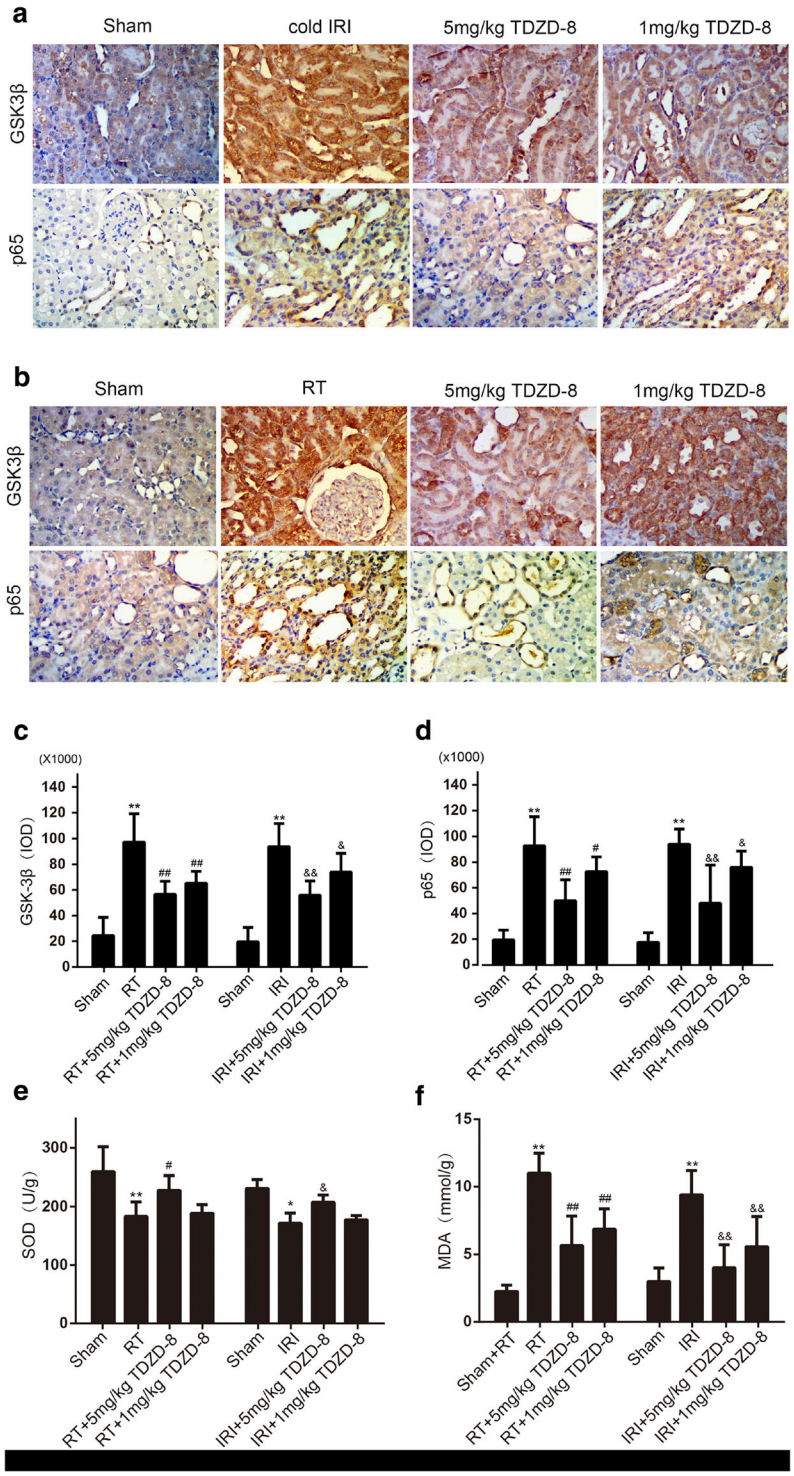

Fig. 8. GSK-3β inhibition reduced oxidative stress injury and the expression of GSK-3β and p65. Expression levels of GSK-3β and p65 in **a** cold IRI model and **b** RT model revealed by IHC. Original magnification × 200. **c**, **d** Integrated optical density (IOD) of GSK-3β and p65 expression in renal tissue. Serum **e** SOD and **f** MDA content in renal tissue of each group. $^{*}P < 0.05$ *vs.* sham group, $^{**}P < 0.01$; $^{\#}P < 0.05$ *vs.* RT group, $^{\#\#}P < 0.01$; $^{\&}P < 0.05$ *vs.* cold IRI group, $^{\&\&}P < 0.01$.

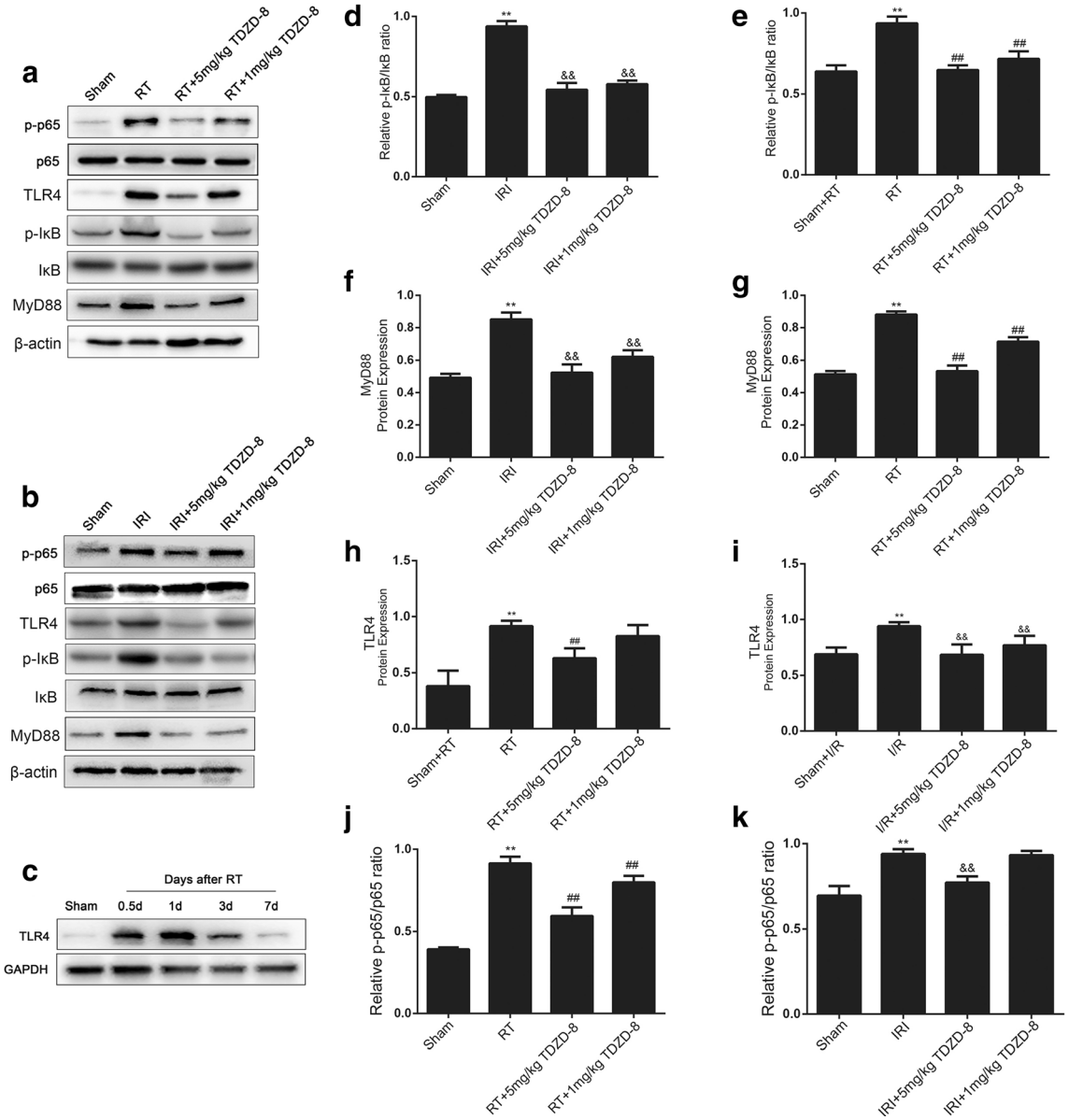

Fig. 9. Effect of GSK-3β inhibitor on expression of the TLR4/MyD88/NF-κB signaling pathway. Expression levels of TLR4, MyD88, p-IκB, IκB, p65, and p-p65 in rat **a** RT and **b** cold IRI models were analyzed 24 h after ischemia-reperfusion. **c** Time-course analysis of renal TLR4 expression. TLR4 expression increased 12 h after IRI, peaked 24 h after IRI, and then decreased gradually. **d**, **e** p-IκB/IκB ratio based on relative band density (RBD) in rat cold IRI and RT models. **f**, **g** Quantitation of RBD for MyD88 in rat cold IRI and RT models. **h**, **i** Quantitation of RBD for TLR4 in rat RT and cold IRI models. **j**, **k** p-p65/p65 ratio based on RBD in rat RT and cold IRI models. $^{*}P < 0.05$ *vs.* sham group, $^{**}P < 0.01$; $^{\#}P < 0.05$ *vs.* RT group, $^{\#\#}P < 0.01$; $^{\&}P < 0.05$ *vs.* cold IRI group, $^{\&\&}P < 0.01$.

MDA content can reflect the oxygen free radical content in tissue and lipid peroxidation level, as well as the ability of such free radicals in tissue damage [44]. Some studies have suggested that IRI increases production of reactive oxygen species (ROS) and levels of MDA while reducing SOD activity [39, 45, 46]. Our study proved that the GSK-3β inhibitor could decrease MDA levels and improve SOD activity, attenuating renal oxidative injury.

CONCLUSION

The GSK-3β inhibitor we investigated, TDZD-8, could inhibit phosphorylation of NF-κB p65 and IκB by inhibiting the TLR/MyD88 pathway, thereby reducing the production of downstream inflammatory factors such as TNF-α, IL-1β, and IL-6. It could also reduce oxidative stress injury, ultimately reducing IRI during KT. In conclusion, our findings suggested that GSK-3β inhibitors in general could serve as new types of inflammatory renal disease modulators and markers and might therefore prove novel therapeutic targets for treating inflammatory injury in KT.

COMPLIANCE WITH ETHICAL STANDARDS

All animal procedures for this study were performed strictly according to the *Guide for the Care and Use of Laboratory Animals* and were approved by the Animal Care and Use Committee of Chongqing Medical University, Chongqing, China.

REFERENCES

1. Collins, A.J., R.N. Foley, C. Herzog, et al. 2013. US Renal Data System 2012 Annual Data Report. *American Journal of Kidney Diseases* 61 (A7): e1–e476.
2. Chen, C.C., W.C. Chapman, and D.W. Hanto. 2015. Ischemia-reperfusion injury in kidney transplantation. *Frontiers in Bioscience (Elite Edition)* 7: 117–134.
3. Foster, M.C., D.E. Weiner, A.G. Bostom, et al. 2017. Filtration markers, cardiovascular disease, mortality, and kidney outcomes in stable kidney transplant recipients: the FAVORIT Trial. *American Journal of Transplantation* 17 (9): 2390–2399.
4. Darrington, R.S., V.M. Campa, M.M. Walker, et al. 2012. Distinct expression and activity of GSK-3α and GSK-3β in prostate cancer. *International Journal of Cancer* 131 (6): E872–E883.
5. Jellestad, L., T. Fink, S. Pradarutti, et al. 2014. Inhibition of glycogen synthase kinase (GSK)-3-beta improves liver microcirculation and hepatocellular function after hemorrhagic shock. *European Journal of Pharmacology* 724: 175–184.
6. Cao, Q., A. Karthikeyan, S.T. Dheen, C. Kaur, and E.A. Ling. 2017. Production of proinflammatory mediators in activated microglia is synergistically regulated by Notch-1, glycogen synthase kinase (GSK-3β) and NF-κB/p65 signalling. *PLoS One* 12 (10): e0186764.
7. O'Neill, S., D. Humphries, G. Tse, et al. 2015. Heat shock protein 90 inhibition abrogates TLR4-mediated NF-κB activity and reduces renal ischemia reperfusion injury. *Scientific Reports* 7 (5): 12958.
8. Feng, R., D. Zhongping, C. Qiao, et al. 2011. The inhibition of glycogen synthase kinase 3 beta ameliorates liver ischemia reperfusion injury via an IL-10-mediated immune regulatory mechanism. *Hepatology.* 54 (2): 687–696.
9. Andrade-Oliveira, V., E.F. Campos, A. Goncalves-Primo, et al. 2012. TLR4 mRNA levels as tools to estimate risk for early post-transplantation kidney graft dysfunction. *Transplantation* 94: 589–595.
10. Marsh, B.J., R.L. Williams-Karnesky, and M.P. Stenzel-Poore. 2009. Toll-like receptor signaling in endogenous neuroprotection and stroke. *Neuroscience.* 158: 1007–1020.
11. Chamorro, A., A. Meisel, A.M. Planas, X. Urra, D. van de Beek, and R. Veltkamp. 2012. The immunology of acute stroke. *Nature Reviews. Neurology* 8: 401–410.
12. Zhang, W.B., H.Y. Zhang, Q. Zhang, et al. 2017. Glutamine ameliorates lipopolysaccharide-induced cardiac dysfunction by regulating the toll-like receptor 4/mitogen-activated protein kinase/nuclear factor-kB signaling pathway. *Experimental and Therapeutic Medicine* 14 (6): 5825–5832.
13. Ratilal, B.O., J.P. Rocha, A.M. Fernandes, et al. 2014. TDZD-8 pretreatment in transient middle cerebral artery occlusion. *Biomedicine and Aging Pathology* 4 (4): 361–367.
14. Spanjol, J., T. Celic, T. Jakljevic, A. Ivancic, and D. Markic. 2011. Surgical technique in the rat model of kidney transplantation. *Collegium Antropologicum* 35: 87–90.
15. Lobb, I., J. Jiang, D. Lian, et al. 2017. Hydrogen sulfide protects renal grafts against prolonged cold ischemia-reperfusion injury via specific mitochondrial actions. *American Journal of Transplantation* 17 (2): 341–352.
16. Ponticelli, C. 2014. Ischaemia-reperfusion injury: a major protagonist in kidney transplantation. *Nephrology, Dialysis, Transplantation* 29 (6): 1134–1140.
17. Cavaillé-Coll, M., S. Bala, E. Velidedeoglu, et al. 2013. Summary of FDA workshop on ischemia reperfusion injury in kidney transplantation. *American Journal of Transplantation* 13 (5): 1134–1148.
18. Guo, F., T. Jiang, W. Song, et al. 2015. Electroacupuncture attenuates cerebral ischemia-reperfusion injury in diabetic mice through adiponectin receptor 1-mediated phosphorylation of GSK-3β. *Molecular Neurobiology* 51 (2): 685–695.
19. Tantray, M.A., I. Khan, H. Hamid, et al. 2016. Synthesis of novel oxazolo [4,5-b]pyridine-2-one based 1,2,3-triazoles as glycogen synthase kinase-3β inhibitors with anti-inflammatory potential. *Chemical Biology & Drug Design* 87 (6): 918–926.
20. Ren, F., Z. Duan, Q. Cheng, et al. 2011. Inhibition of glycogen synthase kinase 3 beta ameliorates liver ischemia reperfusion injury by way of an interleukin-10-mediated immune regulatory mechanism. *Hepatology* 54 (2): 687–696.
21. He, M., Y. Zhang, F. Xie, X. Dou, M. Han, and H. Zhang. 2018. Role of PI3K/Akt/NF-κB and GSK-3β pathways in the rat model of cardiopulmonary bypass-related lung injury. *Biomedicine & Pharmacotherapy* 106: 747–754.
22. Guo, Y., J. Zhang, X. Lai, M. Chen, and Y. Guo. 2018. Tim-3 exacerbates kidney ischaemia/reperfusion injury through the TLR-4/NF-κB signalling pathway and an NLR-C4 inflammasome activation. *Clinical and Experimental Immunology* 193 (1): 113–129.
23. Kim, E., H.C. Kim, S. Lee, et al. 2017. Dexmedetomidine confers neuroprotection against transient global cerebral ischemia/reperfusion injury in rats by inhibiting inflammation through inactivation of the TLR-4/NF-κB pathway. *Neuroscience Letters* 649: 20–27.
24. Feng, D., Y. Wang, Y. Liu, et al. 2018. DC-SIGN reacts with TLR-4 and regulates inflammatory cytokine expression via NF-κB activation in renal tubular epithelial cells during acute renal injury. *Clinical and Experimental Immunology* 191 (1): 107–115.

25. Wu, Huiling, Gang Chen, R. Kate, et al. 2007. TLR4 activation mediates kidney ischemia/reperfusion injury. *The Journal of Clinical Investigation* 117 (10): 2847–2859.
26. Damman, J., et al. 2011. Crosstalk between complement and Toll-like receptor activation in relation to donor brain death and renal ischemia-reperfusion injury. *American Journal of Transplantation* 11: 660–669.
27. Zhang, J., P. Yu, M. Chen, Q. Peng, Z. Wang, and N. Dong. 2017. Remote ischaemic preconditioning and sevoflurane postconditioning synergistically protect rats from myocardial injury induced by ischemia and reperfusion partly via inhibition TLR4/MyD88/NF-kappaB signaling pathway. *Cellular Physiology and Biochemistry* 41: 22–32.
28. Dugo, L., M. Abdelrahman, O. Murch, E. Mazzon, S. Cuzzocrea, and C. Thiemermann. 2006. Glycogen synthase kinase-3β inhibitors protect against the organ injury and dysfunction caused by hemorrhage and resuscitation. *Shock* 25 (5): 485–491.
29. Zhang, F., C.J. Phiel, L. Spece, N. Gurvich, and P.S. Klein. 2003. Inhibitory phosphorylation of glycogen synthase kinase-3 (GSK-3) in response to lithium. Evidence for autoregulation of GSK-3. *The Journal of Biological Chemistry* 278: 33067–33077.
30. Ko, R., and S.Y. Lee. 2016. Glycogen synthase kinase 3β in Toll-like receptor signaling. *BMB Reports* 49 (6): 305–310.
31. Marko, L., E. Vigolo, and C. Hinze. 2016. Tubular epithelial NF-KB activity regulates ischemic AKI. *Journal of the American Society of Nephrology* 27 (9): 2658–2669.
32. Cortes-Vieyra, R., A. Bravo-Patino, J.J. Valdez-Alarcon, M.C. Juarez, B.B. Finlay, and V.M. Baizabal-Aguirre. 2012. Role of glycogen synthase kinase-3 beta in the inflammatory response caused by bacterial pathogens. *Journal of Inflammation* 9 (1): 23–31.
33. Schwabe, R.F., and D.A. Brenner. 2002. Role of glycogen synthase kinase-3 in TNF-a-induced NF-κB activation and apoptosis in hepatocytes. *American Journal of Physiology. Gastrointestinal and Liver Physiology* 283: 204–211.
34. Xu, J., P. Xu, Z. Li, L. Xiao, and Z. Yang. 2013. The role of glycogen synthase kinase-3β in glioma cell apoptosis induced by remifentanil. *Cellular & Molecular Biology Letters* 18 (4): 494–506.
35. Kimura, T., Y. Isaka, and T. Yoshimori. 2017. Autophagy and kidney inflammation. *Autophagy* 13 (6): 997–1003.
36. Schachtner, T., M. Stein, A. Sefrin, N. Babel, and P. Reinke. 2014. Inflammatory activation and recovering BKV-specific immunity correlate with self-limited BKV replication after renal transplantation. *Transplant International* 27 (3): 290–301.
37. Obligado, S.H., O. Ibraghimov-Beskrovnaya, A. Zuk, L. Meijer, and P.J. Nelson. 2008. CDK/GSK-3 inhibitors as therapeutic agents for parenchymal renal diseases. *Kidney International* 73 (6): 684–690.
38. Chhabra, M., T.M. Conlon, K. Saeb-Parsy, and G.J. Pettigrew. 2013. BAFF and associated TNF superfamily members in renal transplantation: an end to BLySful ignorance. *Transplantation* 96 (10): 853–859.
39. Li, Y., D.D. Zhong, L. Lei, Y.L. Jia, H. Zhou, and B.X. Yang. 2015. Propofol prevents renal ischemia-reperfusion injury via inhibiting the oxidative stress pathways. *Cellular Physiology and Biochemistry* 37 (1): 14–26.
40. Zhao, W., X. Gan, G. Su, et al. 2014. The interaction between oxidative stress and mast cell activation plays a role in acute lung injuries induced by intestinal ischemia-reperfusion. *The Journal of Surgical Research* 187 (2): 542–552.
41. Qiao, X., R.S. Li, H. Li, et al. 2013. Intermedin protects against renal ischemia-reperfusion injury by inhibition of oxidative stress. *American Journal of Physiology. Renal Physiology* 304 (1): F112–F119.
42. Jha, J.C., C. Banal, B.S. Chow, M.E. Cooper, and K. Jandeleit-Dahm. 2016. Diabetes and kidney disease: role of oxidative stress. *Antioxidants & Redox Signaling* 25 (12): 657–684.
43. Li, X.D., G.F. Sun, W.B. Zhu, and Y.H. Wang. 2015. Effects of high intensity exhaustive exercise on SOD, MDA, and NO levels in rats with knee osteoarthritis. *Genetics and Molecular Research* 14 (4): 12367–12376.
44. Abd-Elsameea, A.A., A.A. Moustaf, and A.M. Mohamed. 2014. Modulation of the oxidative stress by metformin in the cerebrum of rats exposed to global cerebral ischemia and ischemia/reperfusion. *European Review for Medical and Pharmacological Sciences* 18 (16): 2387–2392.
45. Hsu, S.P., C.C. Chen, and C.T. Chien. 2016. Pretreatment of sialic acid efficiently prevents lipopolysaccharide-induced acute renal failure and suppresses tlr4/gp91-mediated apoptotic signaling. *Kidney & Blood Pressure Research* 41: 267–277.
46. Jung, M., A. Sola, J. Hughes, et al. 2012. Infusion of IL-10-expressing cells protects against renal ischemia through induction of lipocalin-2. *Kidney International* 81: 969–982.